STUDY ON ADAPTIVE MESH GENERATION METHOD IN CFD CALCULATION WITH CONJUGATE HEAT TRANSFER MODEL

IMANO Masashi[1], KAMATA Motoyasu[1], KURABUCHI Takashi[2],
HAYAMA Hirofumi[3], KISHITA Manabu[4]

[1] The University of Tokyo, Tokyo, 113-8685, Japan
[2] Science University of Tokyo, Tokyo, 162-8601, Japan
[3] Hokkaido University, Sapporo, 060-8628, Japan
[4] NTT Power and Building Facilities INC., Tokyo, 180-0012, Japan

ABSTRACT

In order to make proper radiative meshes with considering thermal distribution on solid surfaces, we investigated the adaptive mesh generation method and performed parametric survey for a threshold which controls subdivision of mesh. With these studies we found that the adaptive mesh generation increase the accuracy of predicting mesh surface temperature and air temperature even if the adaptive subdivision is rather soft one. We performed the transient simulation during eight hours after the air-cooling system's breakdown with the mesh generated by the middle adaptive subdivision and compared with the experiment data. As a result the overall agreement between the two was good enough for our practical use.

INTRODUCTION

With the recent advance of high-information-oriented society, a communication equipment has increasingly advanced it's feature, that is high-density and high-heat-generation, so heat generation rate of the room accommodating these equipments tends to increase more and more. Consequently if the air-cooling system at the communication equipment room breaks down due to a disaster or an accident, there is high risk of having communication trouble caused by error or break of a computer inside the equipments, because room air temperature or suction temperature of equipments might suddenly increase. For the purpose of studying the characteristic of air temperature rise affected by the shape of the room and the arrangement of equipment, we have performed CFD(Computer Fluid Dynamics) analysis in which radiation, solid conduction and air convection are conjugated (IMANO 1996). In this paper we newly use the adaptive mesh generation method in the process of dividing solid surfaces into meshes, which is needed for radiation heat transfer calculation. By this method we subdivide the meshes into quarters when those thermal distributions are large. We performed parametric survey for a threshold which controls the subdivision. In addition to that, we carried out the transient simulation and compared the calculated results with full-sized experiment data measured before this simulation.

ADAPTIVE MESH GENERATION

In order to calculate radiative heat transfer among solid surfaces, we must divide solid surfaces into meshes. Since dimension of the Gebhart absorption factors required for the radiation heat transfer calculation equals to the number of the meshes, there is a certain limit in number of the meshes to handle. Consequently we have to generate well-balanced meshes from the viewpoint of their number and resolution with considering thermal distribution on solid surfaces. However we tend to perform the mesh generation without so much care to the thermal distribution because it is difficult to know the distribution before CFD computation. To avoid the dilemma we use adaptive mesh generation method widely used in a field of Computer Graphics for capturing a boundary of shade more sharply. In this method, we first calculate thermal distribution with initial rough meshes. After that subdivisions of meshes are repeated until a difference between the calculated temperature at neighboring meshes is smaller than a preset threshold. In this paper we investigate the effectiveness of this adaptive mesh generation method for the radiation heat transfer calculation.

Methodology

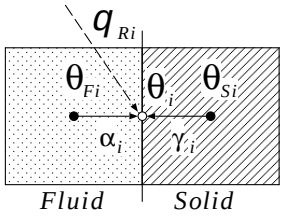

Figure 1: Heat balance at the solid surface

Consider that radiant heat q_{Ri} is passing through the solid surface as shown in Figure 1, the heat balance equation at the surface is expressed as:

$$\alpha_i(\theta_{Fi} - \theta_i) + \gamma_i(\theta_{Si} - \theta_i) + q_{Ri} = 0 \qquad (1)$$

where the radiant heat q_{Ri} is modeled as:

$$q_{Ri} = \sigma\varepsilon_i \sum_j B_{ij} \left(T_j^4 - T_i^4\right)$$

Therefore solid surface temperature θ_i is obtained from Equation (1) as:

$$\theta_i = \frac{\alpha_i \theta_{Fi} + \gamma_i \theta_{Si} + q_{Ri}}{\alpha_i + \gamma_i} \tag{2}$$

As a radiative mesh is normally connected with several fluid or solid cells as shown in Figure 2, we use the area weighted average of temperature at the connected cells as θ_{Fi} or θ_{Si} in Equation(2).

$$\theta_{Fi} = \sum_l \theta_{Fi,l} A_{i,l}/A_i \ , \quad \theta_{Si} = \sum_l \theta_{Si,l} A_{i,l}/A_i$$

Supposing that the radiant heat q_{Ri} is uniform on one mesh, we can guess a temperature on each cell's surface if we use temperature at each cell such as $\theta_{Fi,l}$ or $\theta_{Si,l}$ instead of the average temperature such as θ_{Fi} or θ_{Si} in Equation(2).

$$\theta_{i,l} = \frac{\alpha_i \theta_{Fi,l} + \gamma_i \theta_{Si,l} + q_{Ri}}{\alpha_i + \gamma_i}$$

We divide the mesh into nearly quarters as shown in Figure 3, when temperature difference between the upper and the lower among each cell's surfaces on the same mesh exceeds a preset threshold as:

$$\frac{\max\{\theta_{i,l}\}_l - \min\{\theta_{i,l}\}_l}{\max\{\theta_i\}_i - \min\{\theta_i\}_i} > \text{threshold} \rightarrow \text{subdivide}$$

where $\max\{\}_i$ stand for the maximum value when subscript i varies inside it's domain.
Incidentally we divide the mesh into half, instead of quarters, when an aspect ratio of the mesh exceeds two. This treatment is needed for not to generate the mesh of which the aspect ratio is too large.

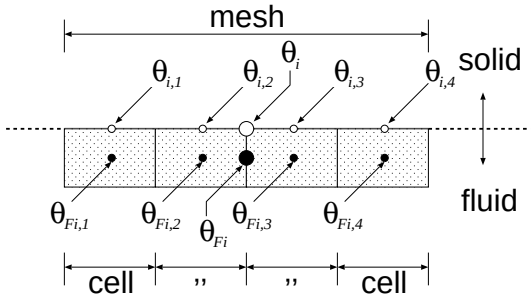

Figure 2: Solid surface mesh and fluid cells

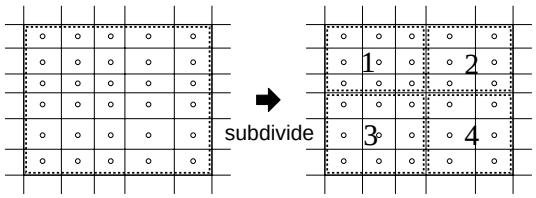

Figure 3: Subdivide a mesh into nearly quarters

Simulation conditions

Simulation conditions in this study are summarized in Table 1. We assume that all surfaces are perfectly diffuse, and the radiation exchange calculations are performed with the Gebhart model. The view factors between the meshes are calculated with Mitalas-Stephenson's line integral method(Walton 1986). Figure 4 shows an outline of a calculation object, boundary conditions and cell divisions. The convective heat transfer coefficients used in these simulations are obtained from an analysis of the full-sized experiment data measured before this simulation. In this study we calculate a flow and thermal distribution in a steady state, so thermal capacity of concrete is set equally to that of air. Table 2 shows simulation cases that varies in the before-mentioned threshold from 20[%] (softest adaptive case) to 0.1[%] (hardest adaptive case). In each cases subdividing of mesh and recalculating flow field and thermal distribution are repeated four times.

Table 1: Simulation conditions

Cell dimension : 80(x)×44(y)×29(z)
Turbulence model : $k-\varepsilon$ (Viollet type)
$C_D = 0.09,\ C_1 = 1.44,\ C_2 = 1.92$
$\sigma_k = 1.0,\ \sigma_\varepsilon = 1.3,\ \sigma_\theta = 0.7$
Navier-Stokes equations solver : SIMPLEC
Simultaneous linear equations solver : CGSTAB
Differential scheme for velocity : QUICK
Differential scheme for scalar : PLDS
Boundary condition for velocity : 1/7 power law
Boundary condition for temperature :
Convective heat transfer coefficients are given
Emissivity of all surfaces : 0.9
Heat generation rate : 0 (i.e. $\theta_{out} = \theta_{in}$)

Table 2: Simulation cases

Threshold [%]	Initial mesh (no adaptive case), 20 (softest adaptive case), 10, 5, 2, 1 (middle adaptive case), 0.5, 0.2, 0.1 (hardest adaptive)

Simulation results

Figure 5 shows the calculated velocity vector field and the air temperature distribution when the threshold equals to 1[%]. Room air temperature is almost 20[°C] at the all region. Initial mesh and generated meshes are shown in Figure 6. In the hardest adaptive case we find that surfaces at the beam or near corner are subdivided into small meshes. Incidentally the temperature width among all surfaces in the initial mesh case equals to 2.6[°C] and it's standard deviation equals to 0.6[°C].

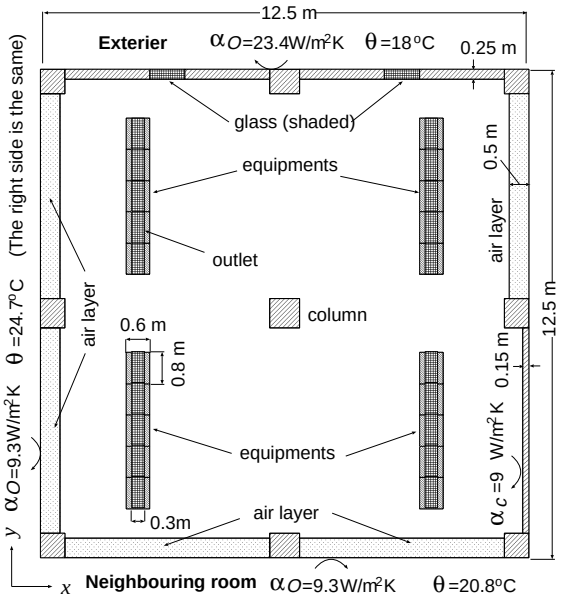

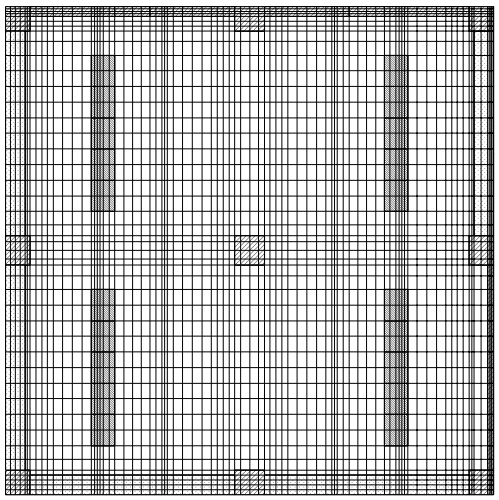

x-y section

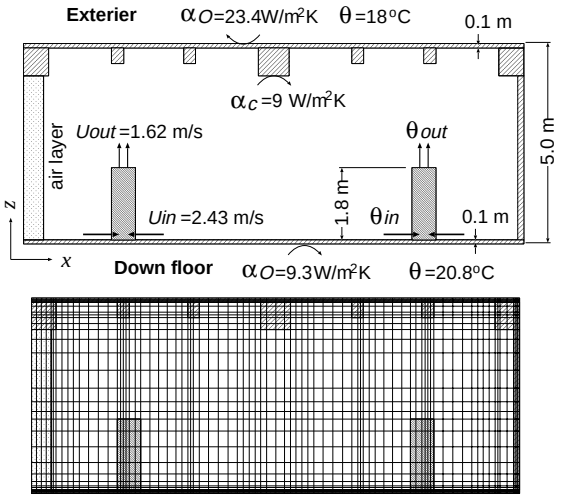

x-z section

Figure 4: Calculation object, boundary conditions and cell divisions

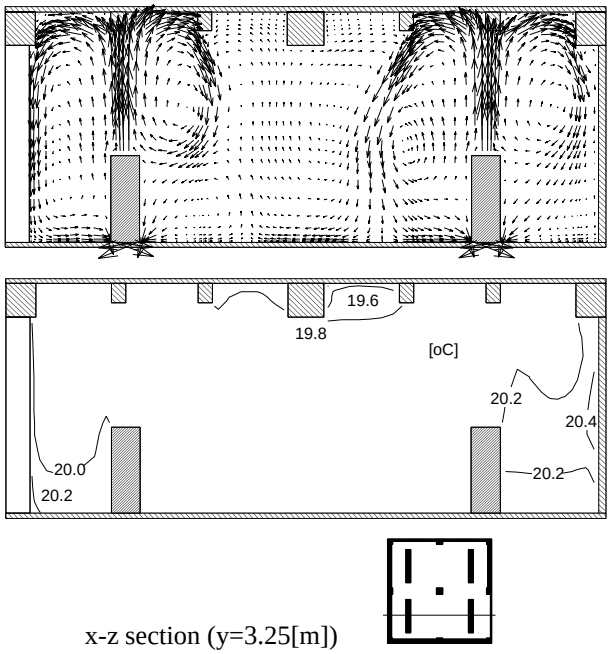

x-z section (y=3.25[m])

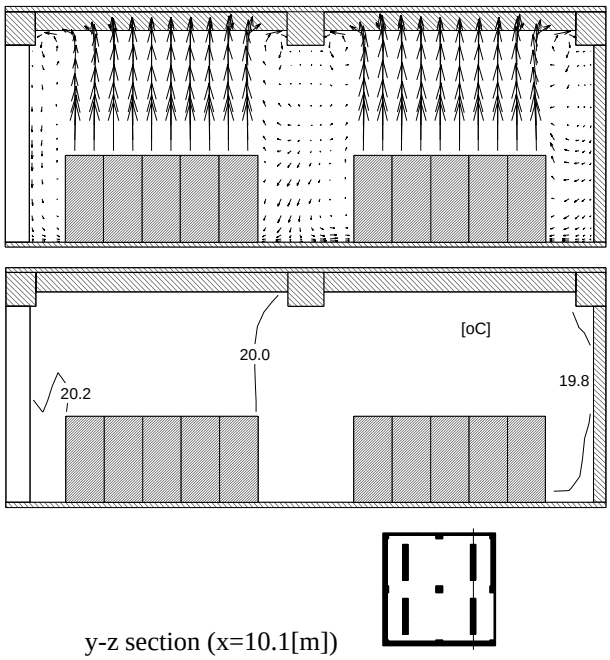

y-z section (x=10.1[m])

Figure 5: Velocity vector field and air temperature distribution when the threshold equals to 1[%]

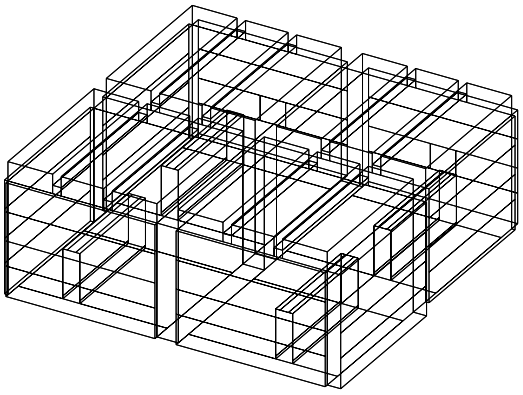

No adaptive case
(Initial meshes)
The number of the meshes is 212.

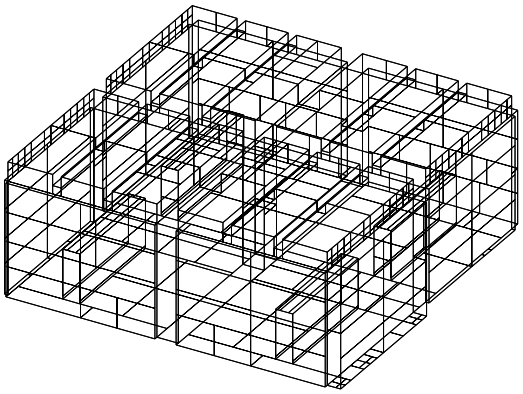

Middle adaptive case
Threshold equals to 1 [%].
The number of the meshes is 491.

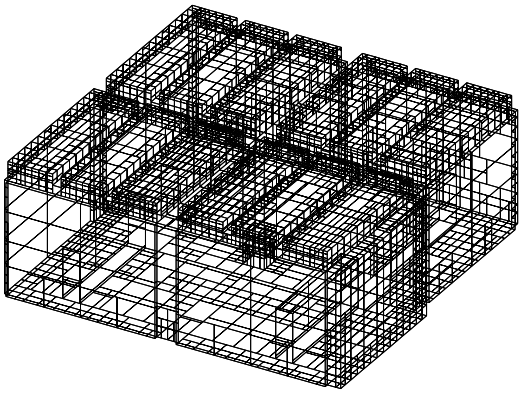

Hardest adaptive case
Threshold equals to 0.1 [%].
The number of the meshes is 4255.

Figure 6: Initial mesh and generated meshes

Analysis

In this analysis the flow and thermal fields obtained with the most fine meshes when the threshold equals to 0.1[%] are regarded as the most precise solution. And we calculate errors about mesh temperature, radiative exchange per unit area and air temperature from the precise solution in each cases. These are shown in Figure 7. Each errors are normalized with each width in the precise solution. The both of maximum and average errors about the mesh temperature and radiative heat exchange are on the slight decrease when the threshold is lager than 1[%]. And they start to fall off when the threshold equals to 1[%]. About the air temperature the error is much small than that in the case of the initial mesh even if the threshold equals to 20[%] and adaptive subdivision is very soft. On the other hand the number of generated meshes increases rapidly when the threshold is below 1[%], so the ratio of it's calculation cost to the improvement of accuracy becomes worth.

Based on the above-mentioned reasons, the middle adaptive case when the threshold is 1[%] is considered as the most suitable case for this object, so the generated mesh in this case is used on the next transient simulation.

TRANSIENT SIMULATION

We carried out the transient simulation during eight hours after the air-cooling system's breakdown. Calculation conditions for this study are summarized in Table 3. Other conditions are the same as in Table 1 and Figure 4. Since thirty minutes after the breakdown, only thermal field is calculated on the assumption that the velocity vector field virtually unchanged.

Figure 8 shows the velocity vector field and the air temperature distribution at thirty minutes after the air-cooling system's breakdown. Similarly Figure 9 and Figure 10 show the air temperature distribution at three hours after and at eight hours after as each.

Figure 11 show a comparison about room air temperature between this simulation and the experiment data. Measured points for air temperature in the experiment are 144 points. Although the simulation results increase more rapidly than the measured data in the initial period, the overall agreement between the two is good enough for our practical use. Because our concern is relatively about the late period when the air temperature is rather high and there is possibility of break or error of a computer inside the equipments.

We knew that this rapid increase is almost due to a lack of grid refinement at the solid cell connected with room surfaces. But if we use the traditional static grid refinement at the solid, cell dimensions rapidly increase and aspect ratio of fluid cells enlarges more. So we intend to solve this problem with the adaptive grid refinement method later rather than the static grid refinement.

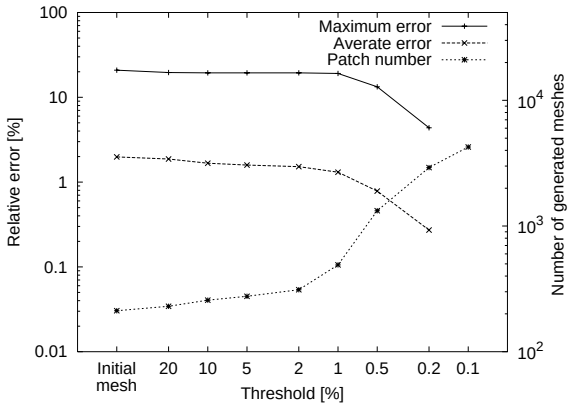

Mesh temperature

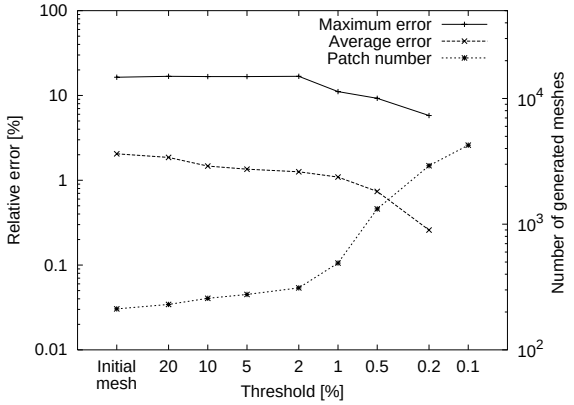

Radiative heat exchange per unit area

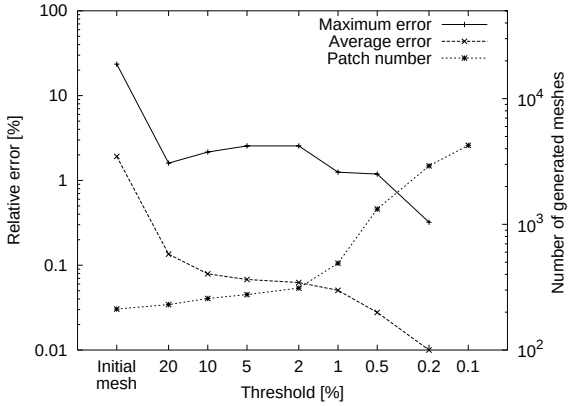

Air temperature

Figure 7: The relative errors about mesh temperature, radiative heat exchange and air temperature from the precise solution

Table 3: Transient simulation conditions

Time divisions :
Δt = 0.1 [s] ($t < 1$ [s])
= 0.2 [s] ($t < 10$ [s])
= 0.5 [s] ($t < 1$ [m])
= 1.0 [s] ($t < 10$ [m])
= 2.0 [s] ($t < 30$ [m])
= 5.0 [s] ($t < 3$ [h], flow is fixed)
= 10 [s] ($t < 8$ [h], flow is fixed)
Heat generation rate : 40 [kW]
: $\theta_{out} = \theta_{in} + 4.286$[°C]

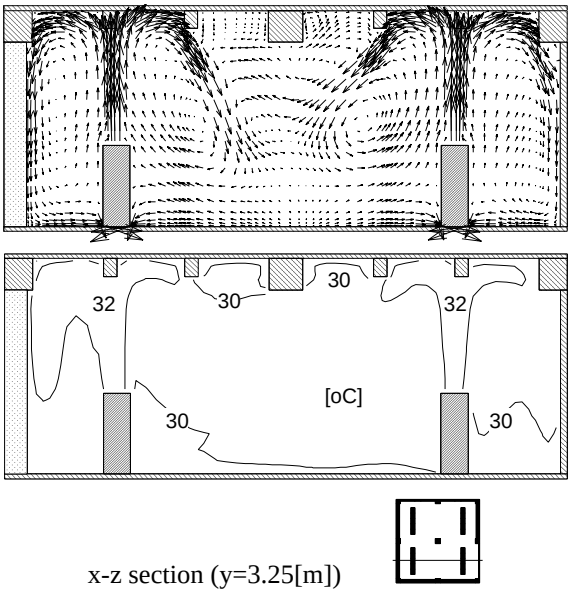

x-z section (y=3.25[m])

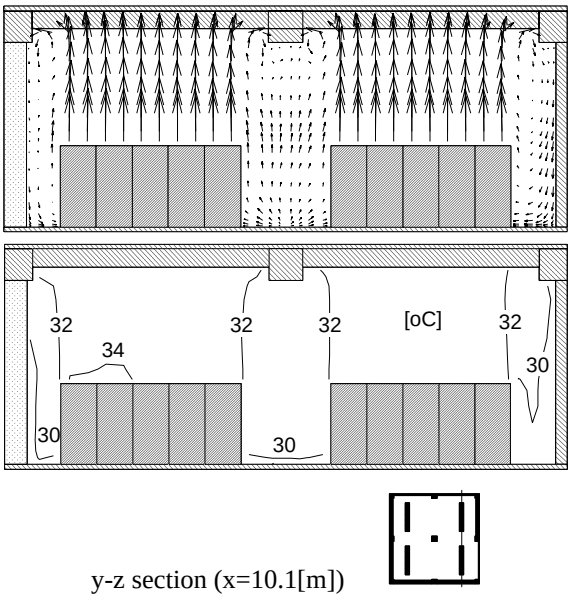

y-z section (x=10.1[m])

Figure 8: Velocity vector field and air temperature distribution thirty minutes after the air-cooling system's breakdown

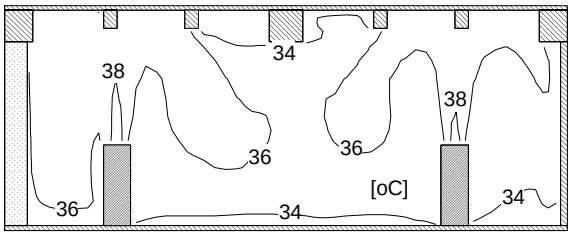

x-z section (y=3.25[m])

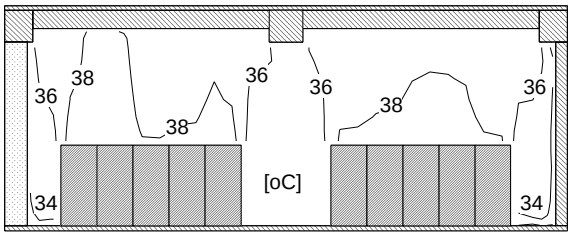

y-z section (x=10.1[m])

Figure 9: Air temperature distribution three hours after the air-cooling system's breakdown

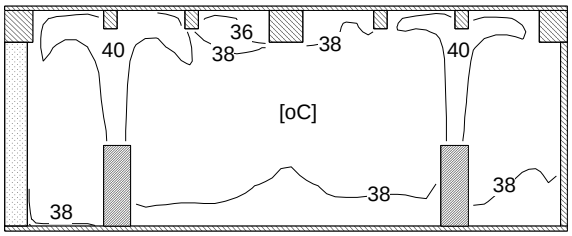

x-z section (y=3.25[m])

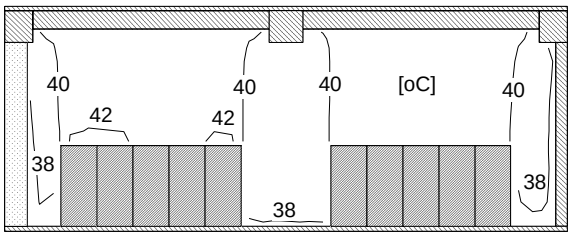

y-z section (x=10.1[m])

Figure 10: Air temperature distribution eight hours after the air-cooling system's breakdown

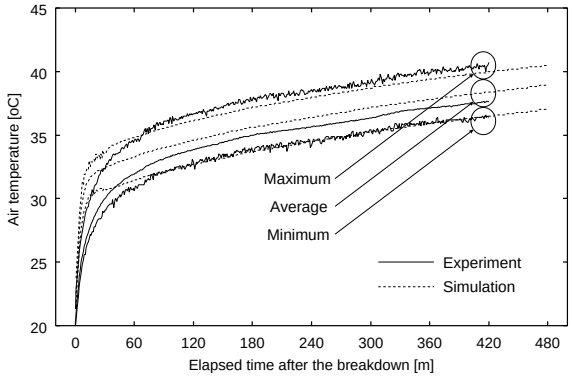

Figure 11: Comparison between experiment and simulation results about room air temperature

CONCLUSIONS

We investigated the adaptive mesh generation method and performed parametric survey for a threshold which controls the subdivision. With these studies we found that the adaptive mesh generation increases the accuracy of predicting the mesh surface temperature or air temperature even if the adaptive subdivision is rather soft one. On the other hand the number of generated meshes increases rapidly in the hard adaptive cases. Therefore the ratio of it's calculation cost to the improvement of accuracy becomes worth. Based on the above-mentioned reasons we adapted the mesh generated by the middle adaptive case and performed the transient simulation during eight hours after the air-cooling system's breakdown. Comparing with the experimental data, the overall agreement between the two was good enough for our practical use.

NOMENCLATURE

α	heat transfer coefficient of the fluid
γ	heat transfer coefficient of the solid
θ_F	temperature at the fluid
θ_S	temperature at the solid
θ_i	temperature at the mesh surface
$\theta_{i,l}$	temperature at the cell surface
q_R	radiative heat flux
σ	Stefan-Boltzmann constant
ε	emissivity
B_{ij}	the Gebhart absorption factors
T	absolute temperature at the mesh surface
A	area of the mesh or cell surface
$\theta_{in/out}$	suction/outlet temperature of the equipment
$U_{in/out}$	suction/outlet velocity of the equipment
α_c	convective heat transfer coefficient
α_o	overall heat transfer coefficient
Δt	time division

ACKNOWLEDGMENT

The authors wish to express our gratitude to Professor Y. Matsuo of Meiji university, Professor Y. Sakamoto of the University of Tokyo and members of Nagare-no-kai for their advice during this work.

REFERENCES

IMANO, M., KURABUCHI, T., KAMATA, M. and HAYAMA H., "A Long Term Transient Analysis of Thermal Flow Field of a Telecommunication Equipment Room in Case of Air-cooling System Breakdown", International Symposium on Room Air Convection and Ventilation Effectiveness, pp.119–126, 1996.

George N. Walton, "Algorithms for Calculating Radiation View Factors Between Plane Convex Polygons with Obstructions", NATIONAL BUREAU OF STANDARDS, 1986.